

Section S1.

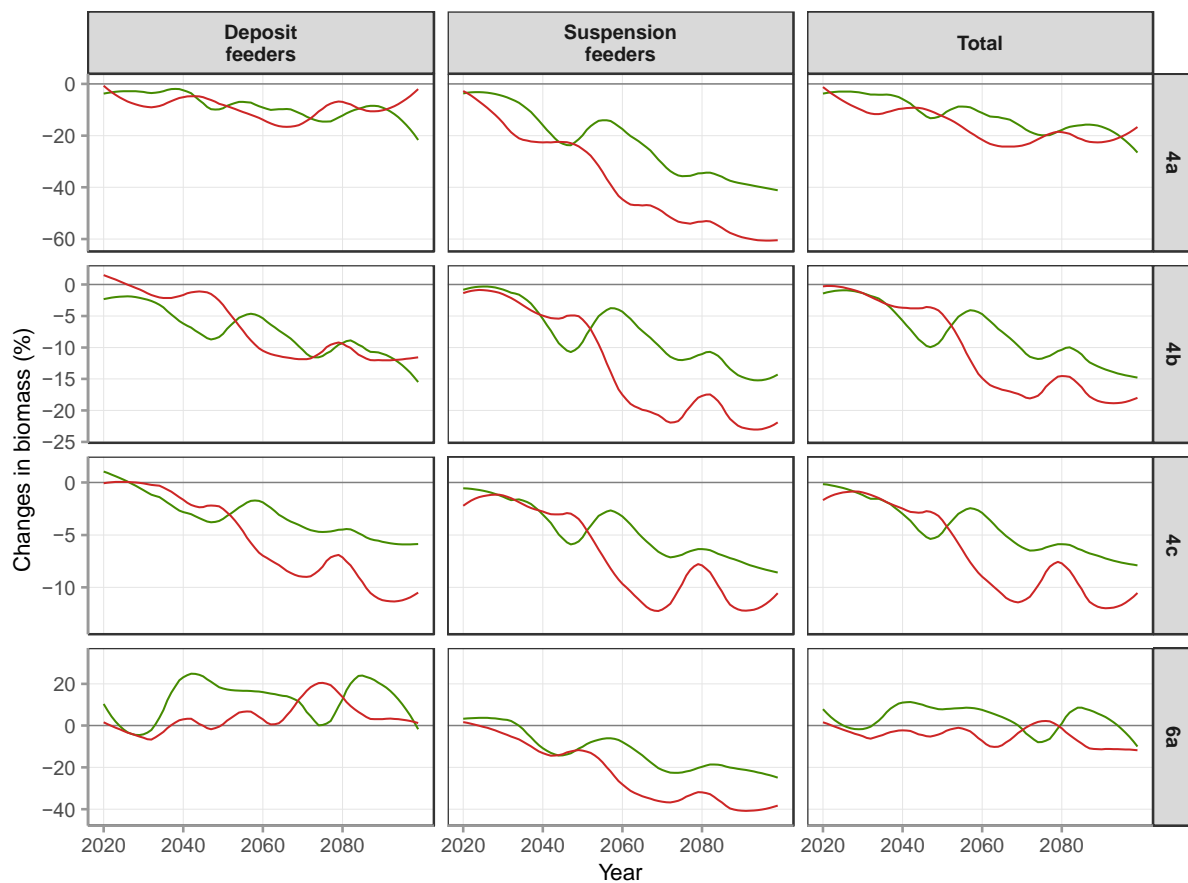


Figure S1.1: Projected changes in biomass of benthic secondary producers between 2020 and 2100 relative to the reference period 2013–2017 for the ICES divisions 4a–c and 6a. The changes in biomass are presented for two scenarios RCP4.5 (green lines) and RCP8.5 (red lines). The smoothing lines are the smoothed trends of the changes.

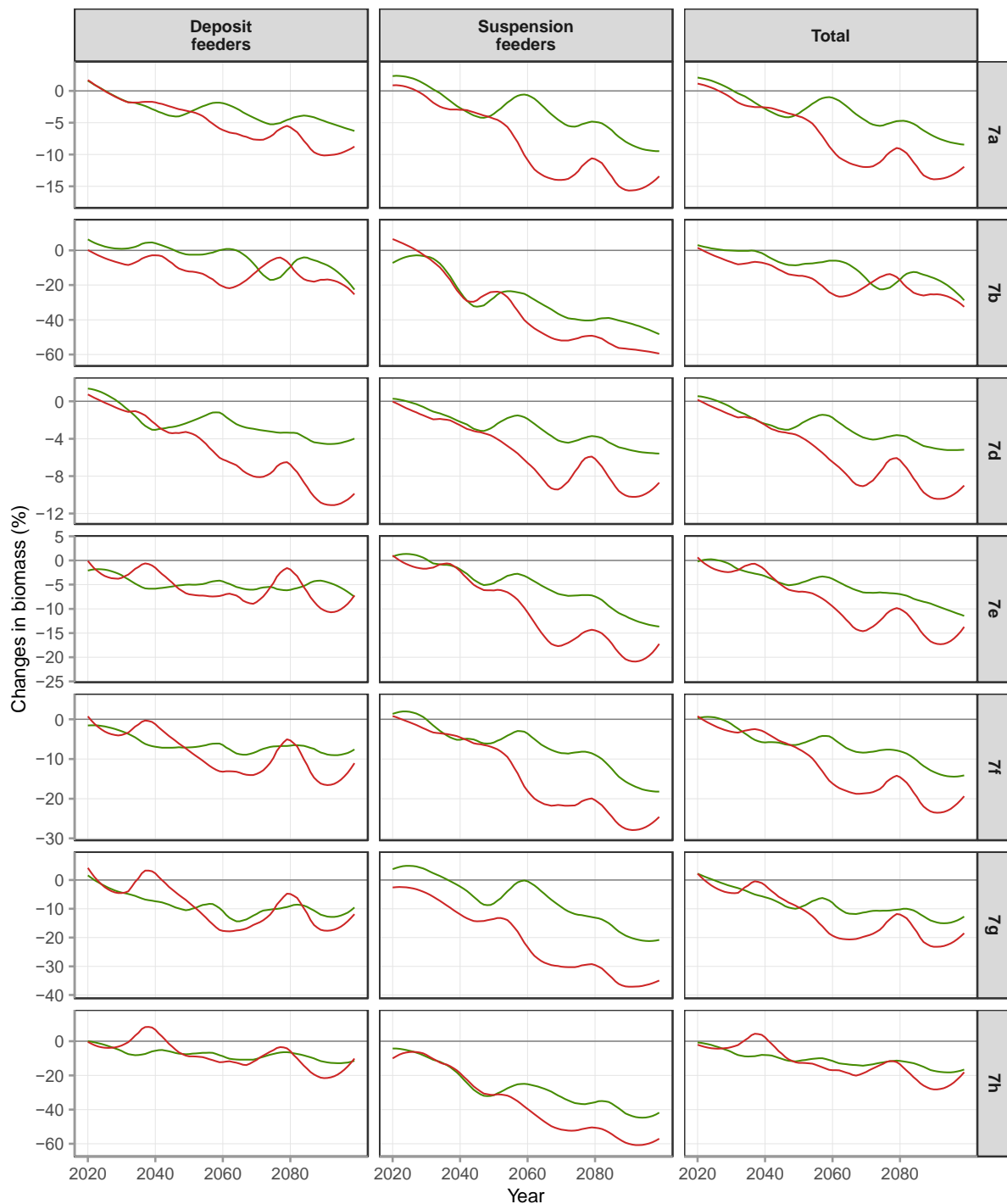


Figure S1.2: Projected changes in biomass of benthic secondary producers between 2020 and 2100 relative to the reference period 2013–2017 for the ICES divisions 7a, b, d, e, f, g, h. The changes in biomass are presented for two scenarios RCP4.5 (green lines) and RCP8.5 (red lines). The smoothing lines are the smoothed trends of the changes.

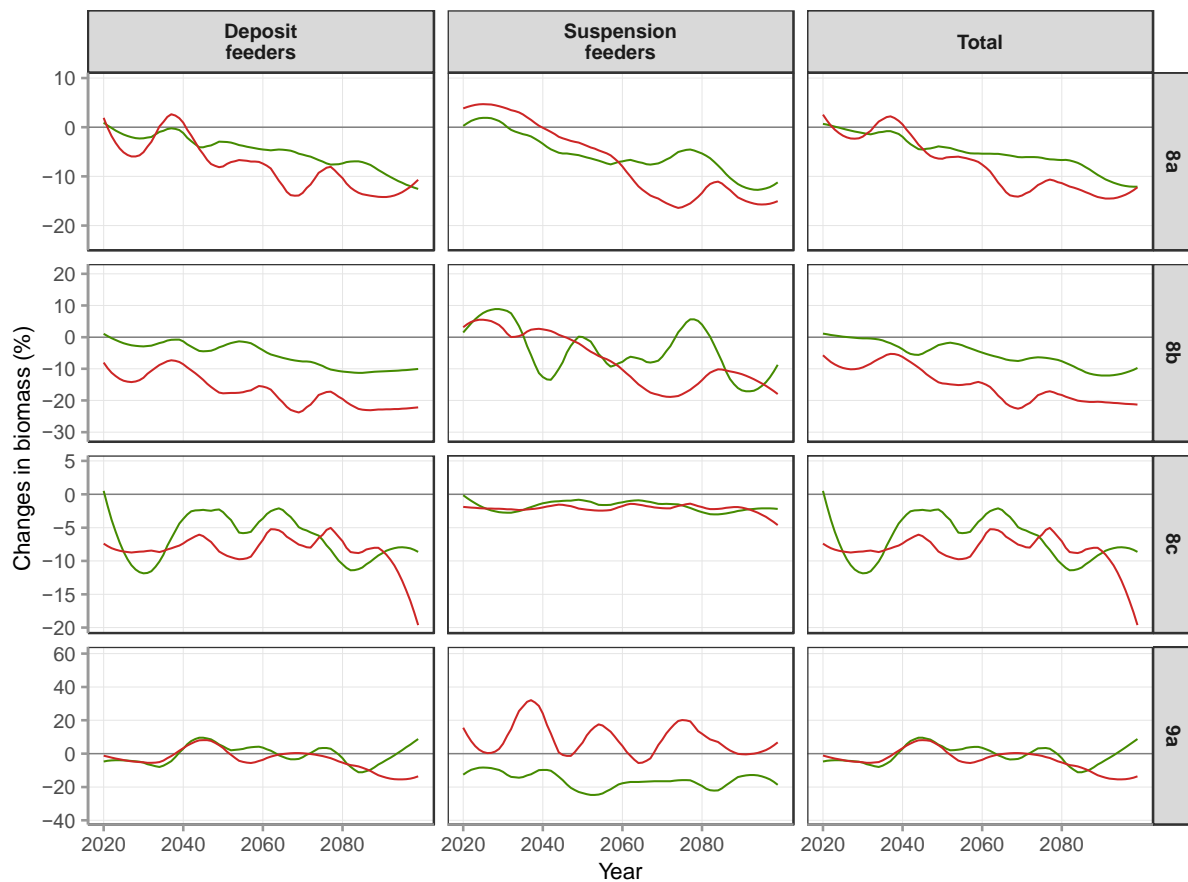


Figure S1.3 :Projected changes in biomass of benthic secondary producers between 2020 and 2100 relative to the reference period 2013-2017 for the ICES divisions 8a-c and 9a. The changes in biomass are presented for two scenarios RCP4.5 (green lines) and RCP8.5 (red lines).

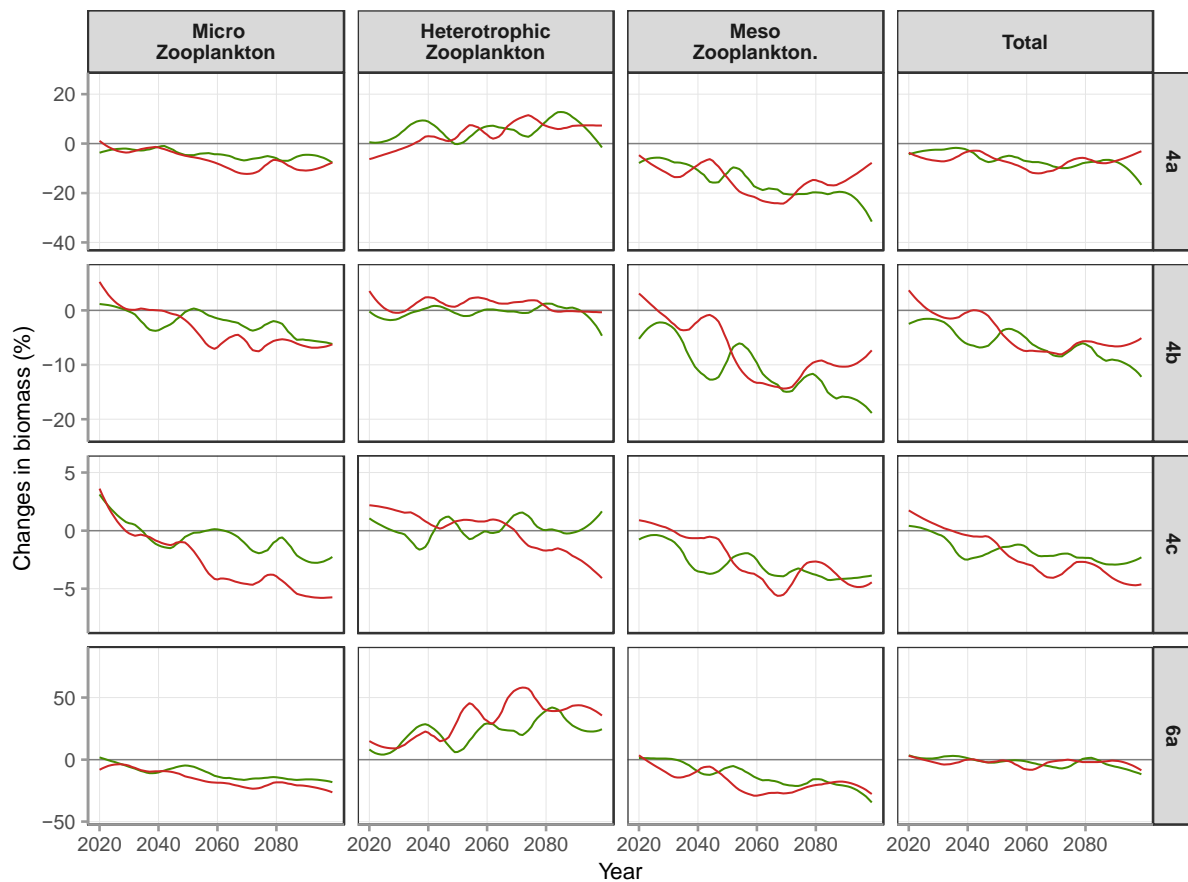


Figure S1.4: Projected changes in biomass of pelagic secondary producers between 2020 and 2100 relative to the reference period 2013–2017 for the ICES divisions 4a-c and 6a. The changes in biomass are presented for two scenarios RCP4.5 (green lines) and RCP8.5 (red lines). The smoothing lines are the smoothed trends of the changes.

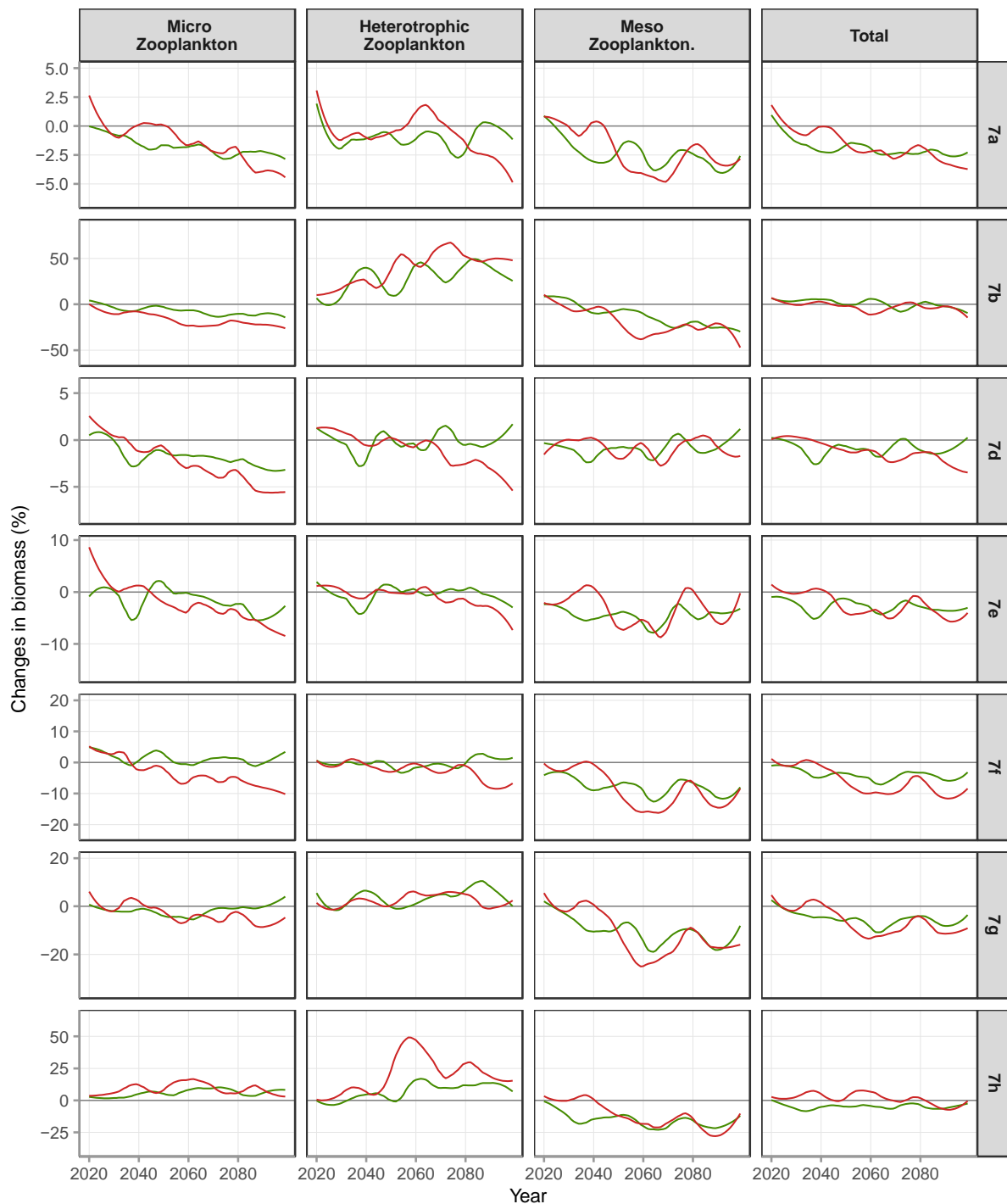


Figure S1.5: Projected changes in biomass of pelagic secondary producers between 2020 and 2100 relative to the reference period 2013–2017 for the ICES divisions 7a, b, d, e, f, g, h. The changes in biomass are presented for two scenarios RCP4.5 (green lines) and RCP8.5 (red lines). The smoothing lines are the smoothed trends of the changes.

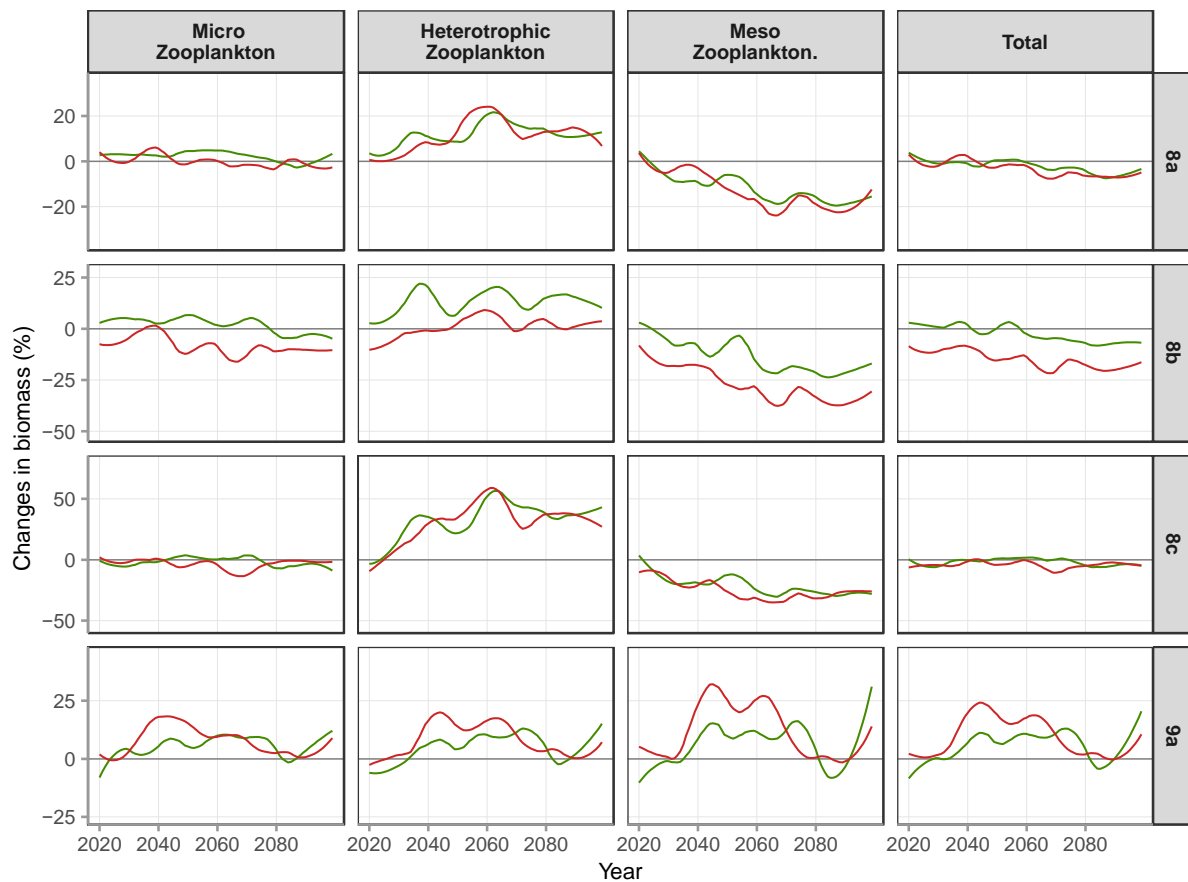


Figure S1.6: Projected changes in biomass of pelagic secondary producers between 2020 and 2100 relative to the reference period 2013-2017 for the ICES divisions 8a-c and 9a. The changes in biomass are presented for two scenarios RCP4.5 (green lines) and RCP8.5 (red lines). The smoothing lines are the smoothed trends of the changes.

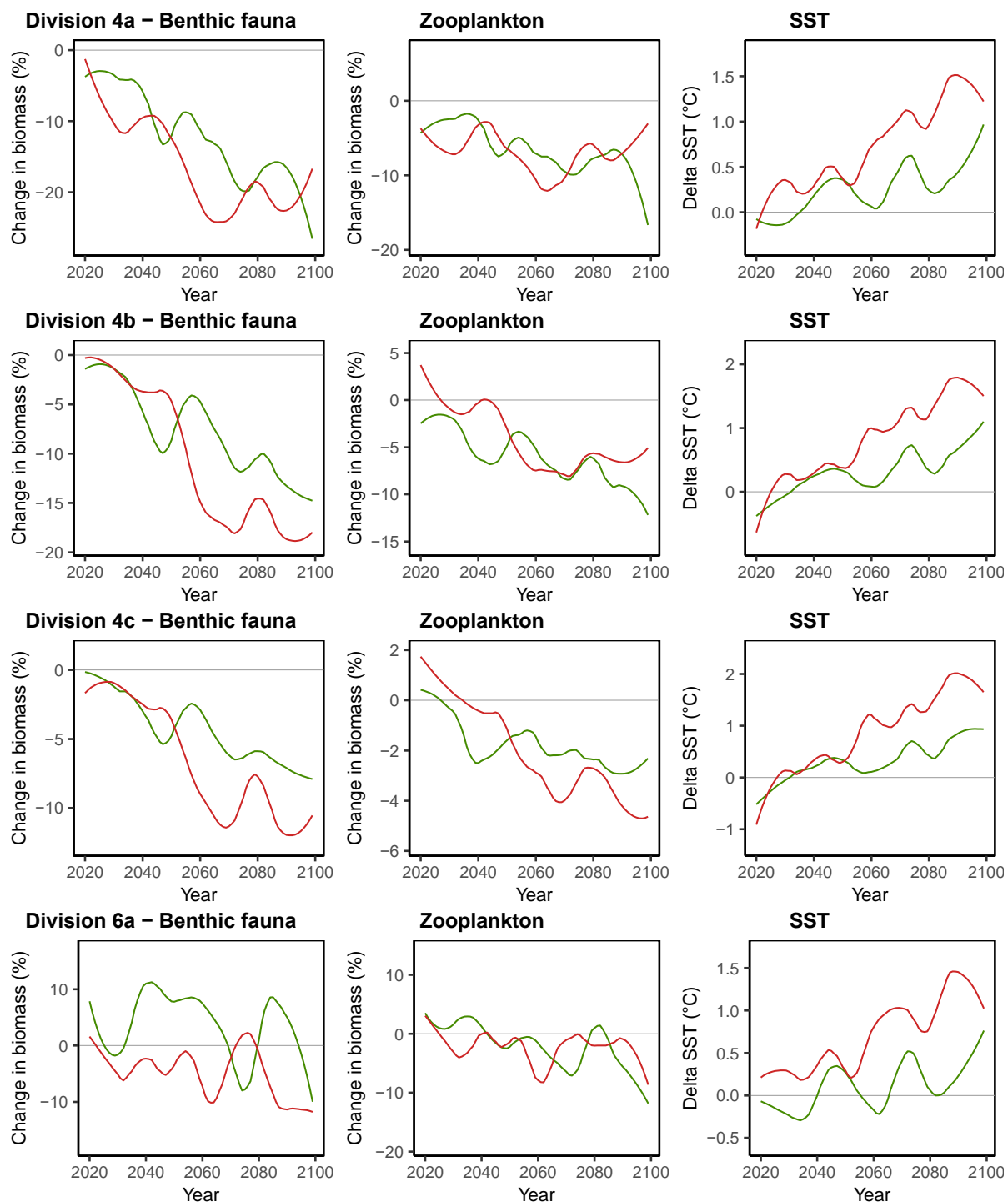


Figure S1.7: Projected changes in biomass of benthic fauna, zooplankton and sea surface temperature between 2020 and 2100 relative to the reference period 2013–2017 for the ICES divisions 4a-c and 6a. The changes in biomass and SST are presented for the two scenarios RCP4.5 (green) and RCP8.5 (red). The smoothing lines are the smoothed trends of the changes.

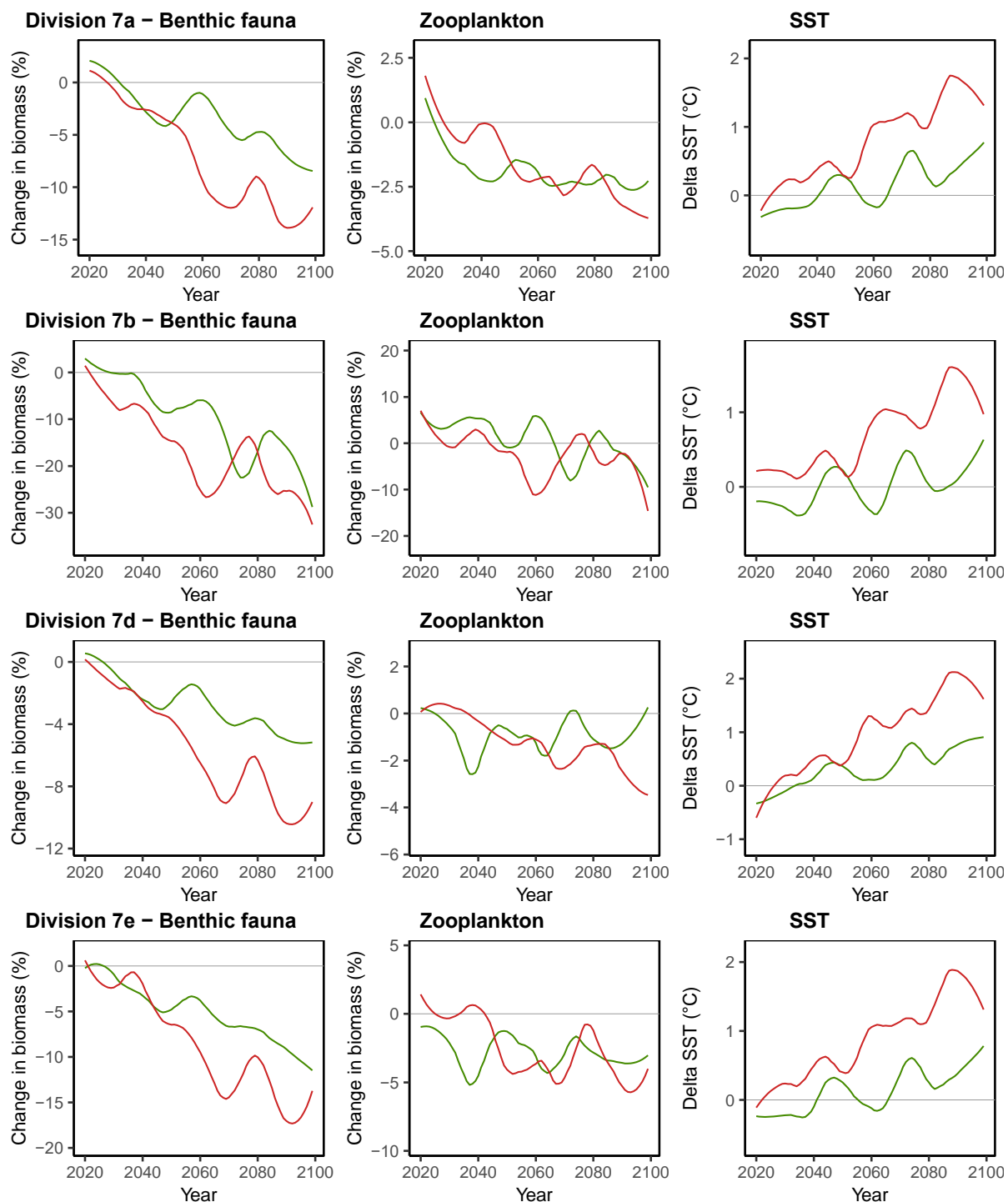


Figure S1.8: Projected changes in biomass of benthic fauna, zooplankton and sea surface temperature between 2020 and 2100 relative to the reference period 2013–2017 for the ICES divisions 7a, b, d, e. The changes in biomass and SST are presented for the two scenarios RCP4.5 (green) and RCP8.5 (red). The smoothing lines are the smoothed trends of the changes.

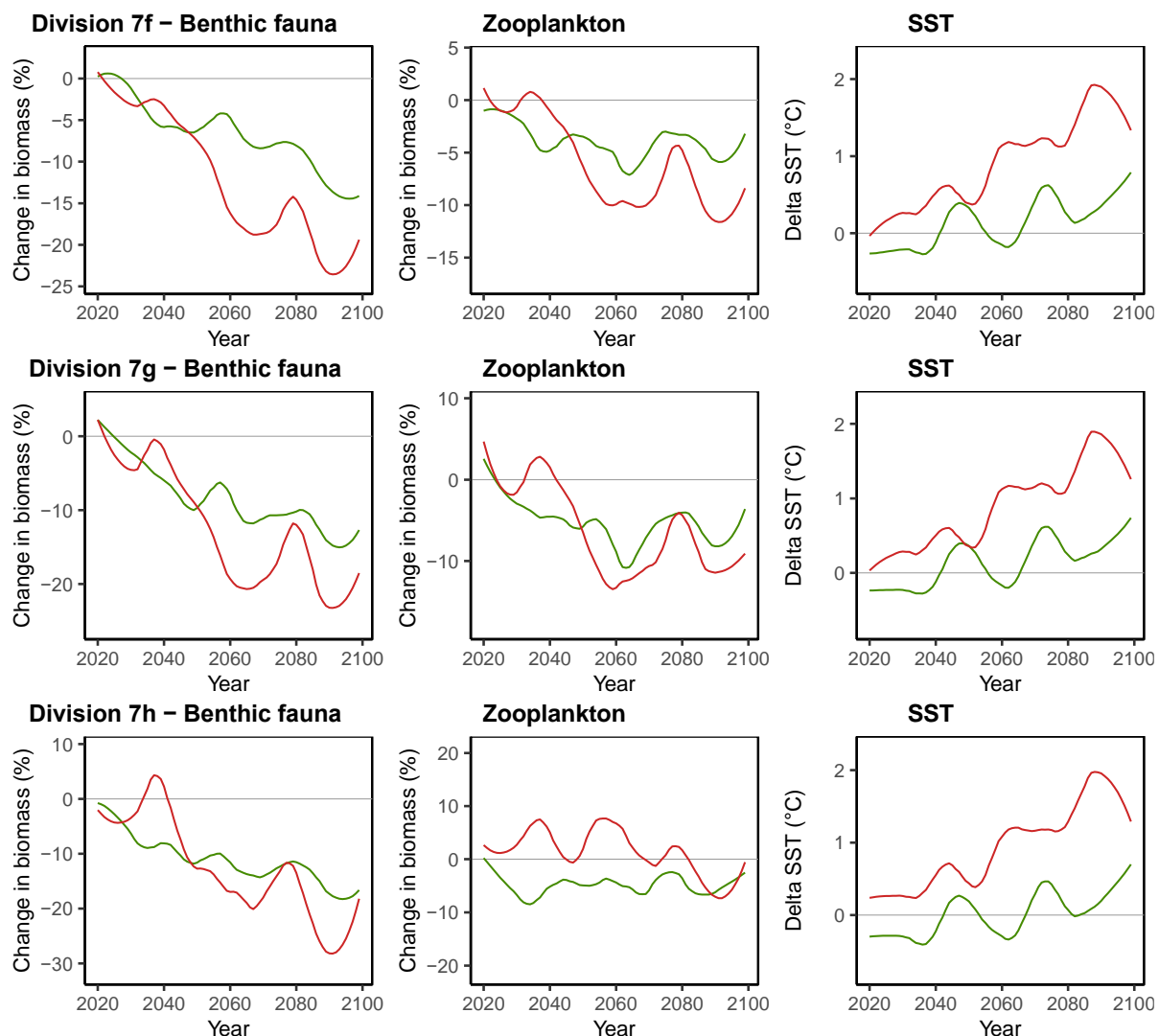


Figure S1.9: Projected changes in biomass of benthic fauna, zooplankton and sea surface temperature between 2020 and 2100 relative to the reference period 2013–2017 for the ICES divisions 7f, g, h. The changes in biomass and SST are presented for the two scenarios RCP4.5 (green) and RCP8.5 (red). The smoothing lines are the smoothed trends of the changes.

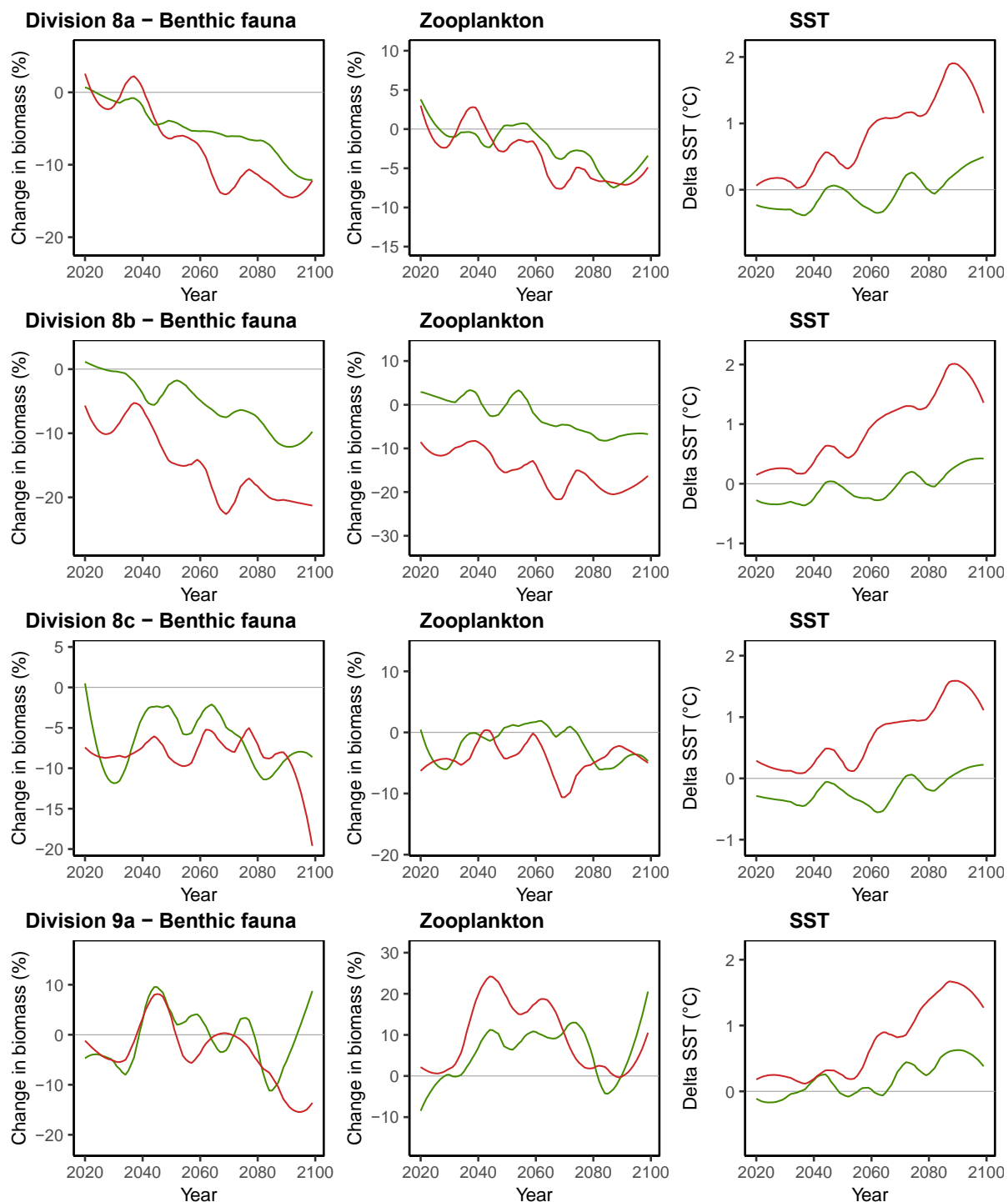


Figure S1.10: Projected changes in biomass of benthic fauna, zooplankton and sea surface temperature between 2020 and 2100 relative to the reference period 2013–2017 for the ICES divisions 8a, b, c and 9a. The changes in biomass and SST are presented for the two scenarios RCP4.5 (green) and RCP8.5 (red). The smoothing lines are the smoothed trends of the changes.

Section S2.

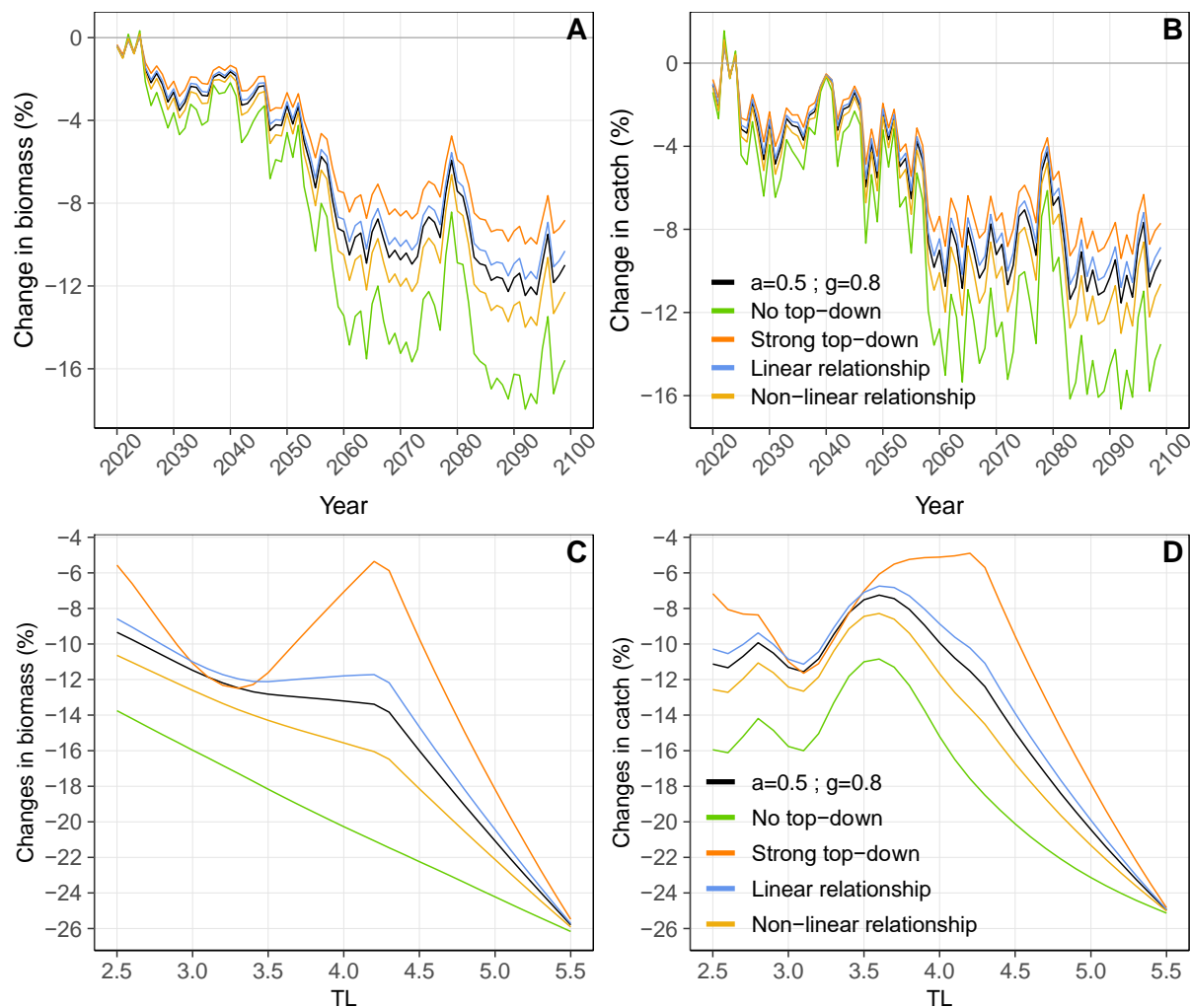


Figure S.2.1: Global projected changes in biomass and catch with different top-down control intensities and predator-prey functional relationships. Panels (A) and (B) represent the projected change in total (between $TL=2.5$ and $TL=5.5$) biomass and catch between 2020 and 2100 relative to the reference period (2013–2017) under RCP8.5. Panels (C) and (D) show the projected changes in biomass and catch at each trophic class in 2090–2099 relative to 2013–2017 under RCP8.5. Note that “ $a=0.5$ and $g=0.8$ ” is the top-down control intensity ($\alpha=0.5$) and predator-prey functional relationship ($\gamma=0.8$), we used in the paper. “Strong top-down” is a model with $\alpha=1$, “Linear relationship” represents the model with a linear predator-prey functional relationship ($\gamma=1$), “Non-linear relationship” the model with a non-linear predator-prey functional relationship ($\gamma=0.5$).

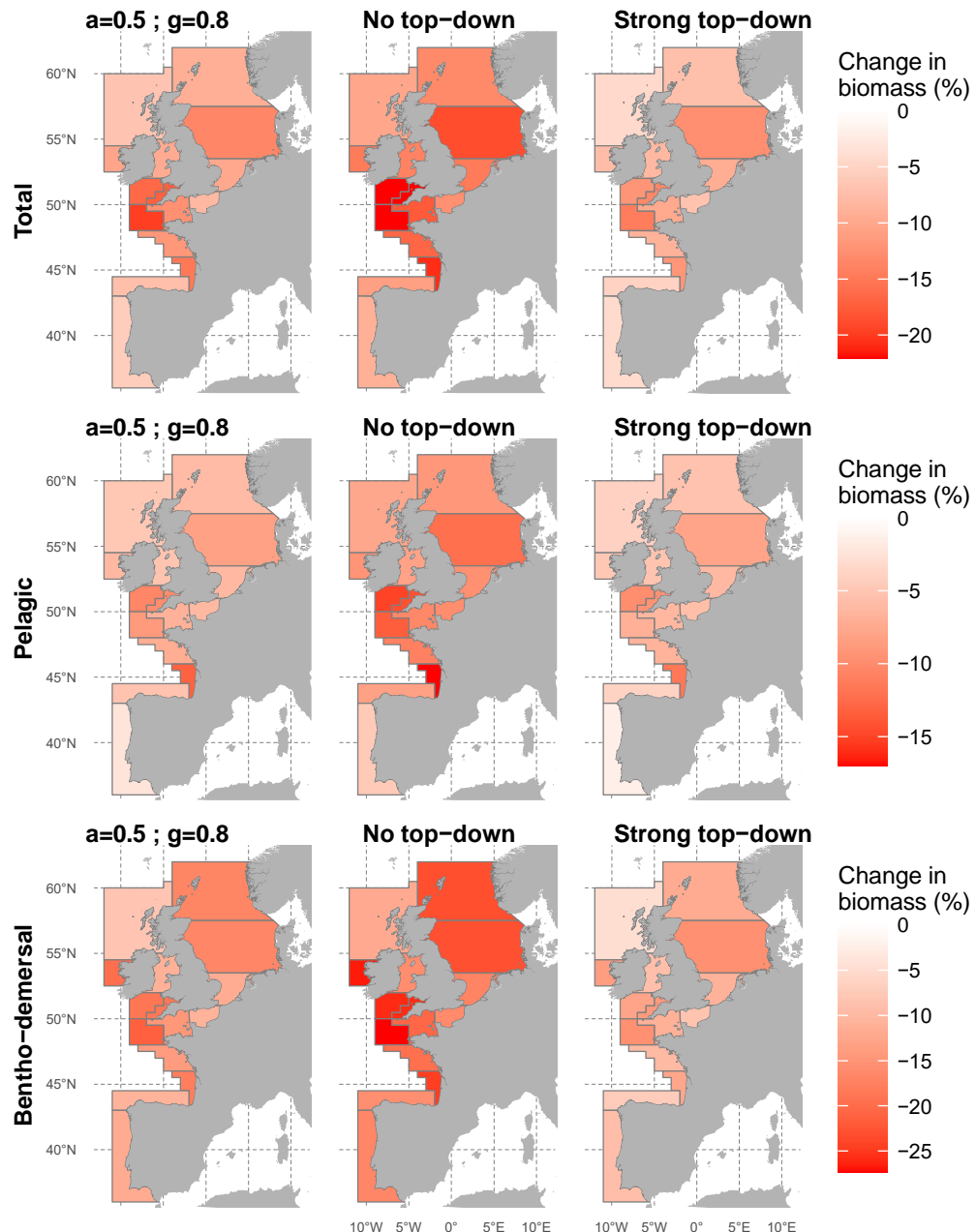


Figure S2.2: Maps of the changes in total biomass in 2090–2099 relative to 2013–2017 under RCP8.5 for different top-down control intensities. The changes in total biomass ($TL \geq 2.5$) were aggregated for the entire ecosystem (top panels), the pelagic ecosystem component (center panels) and the benthic-demersal ecosystem component (bottom panels). Each column represents a top-down control intensity. Note that “ $a=0.5$ and $g=0.8$ ” is the top-down control intensity ($\alpha=0.5$) and predator-prey functional relationship ($\gamma=0.8$), we used in the paper.

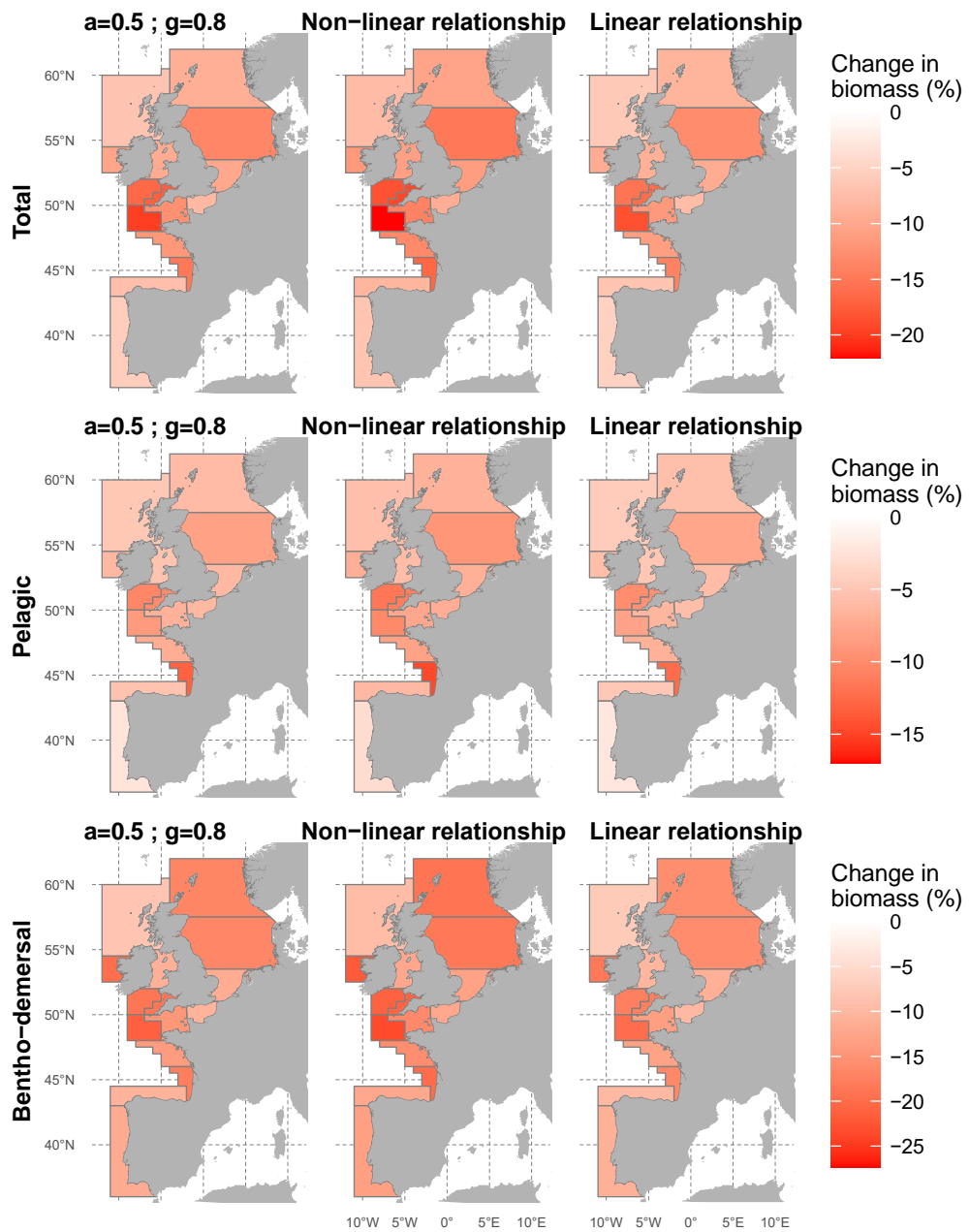


Figure S2.3: Maps of the changes in total biomass in 2090–2099 relative to 2013–2017 under RCP8.5 for different predator-prey functional relationships in the top-down control function. The changes in total biomass ($TL \geq 2.5$) were aggregated for the entire ecosystem (top panels), the pelagic ecosystem component (center panels) and the benthic-demersal ecosystem component (bottom panels). Each column represents a top-down control intensity. Note that “ $a = 0.5$ and $g = 0.8$ ” is the top-down control intensity ($\alpha = 0.5$) and predator-prey functional relationship ($\gamma = 0.8$), we used in the paper, “Linear relationship” represents the model with a linear predator-prey functional relationship ($\gamma = 1$) and “Non-linear relationship” the model with a non-linear predator-prey functional relationship ($\gamma = 0.5$).

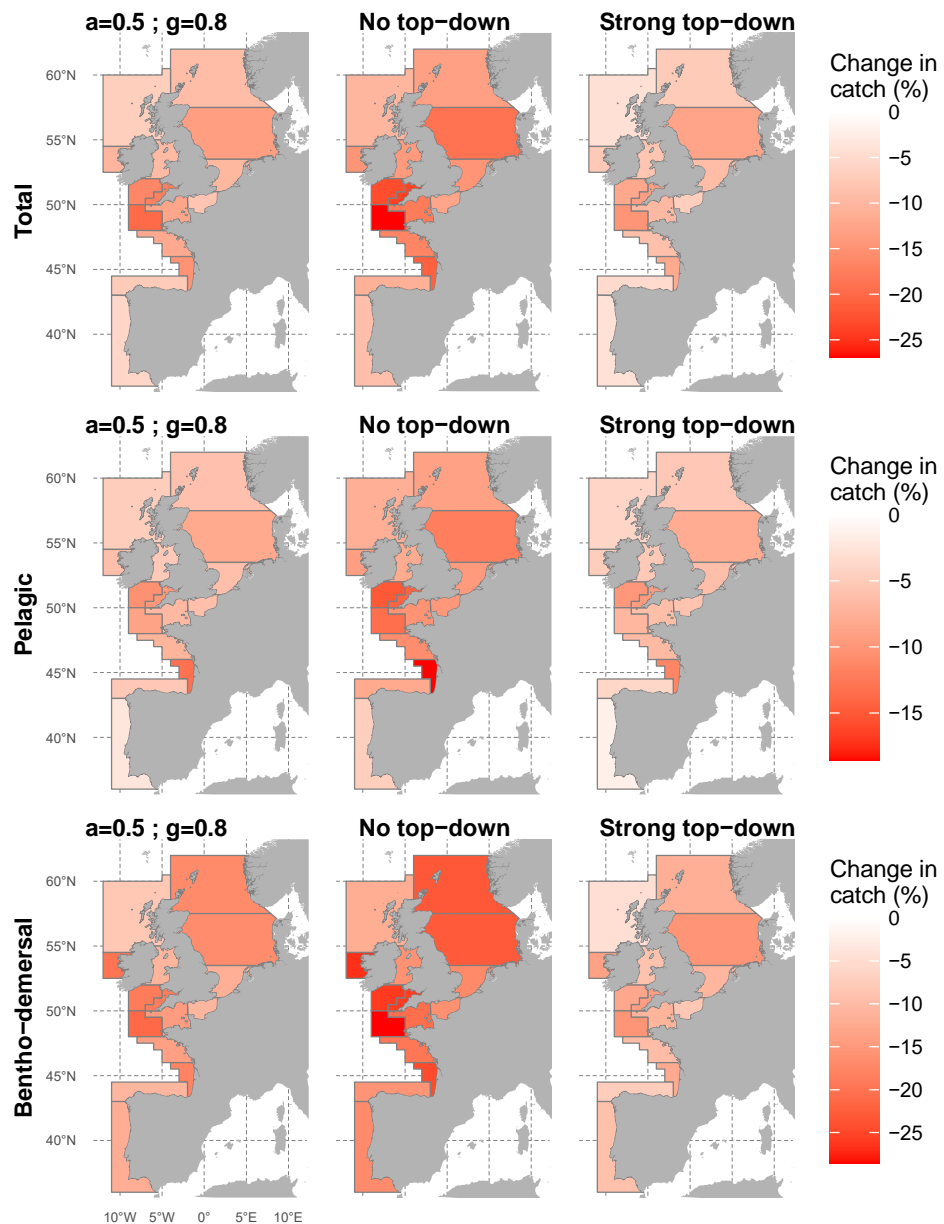


Figure S2.4: Maps of the changes in total catch in 2090–2099 relative to 2013–2017 under RCP8.5 for different top-down control intensities. The changes in total catch ($TL \geq 2.5$) were aggregated for the entire ecosystem (top panels), the pelagic ecosystem component (center panels) and the benthic-demersal ecosystem component (bottom panels). Each column represents a top-down control intensity. Note that “ $a = 0.5$ and $g = 0.8$ ” is the top-down control intensity ($\alpha = 0.5$) and predator-prey functional relationship ($\gamma = 0.8$), we used in the paper.

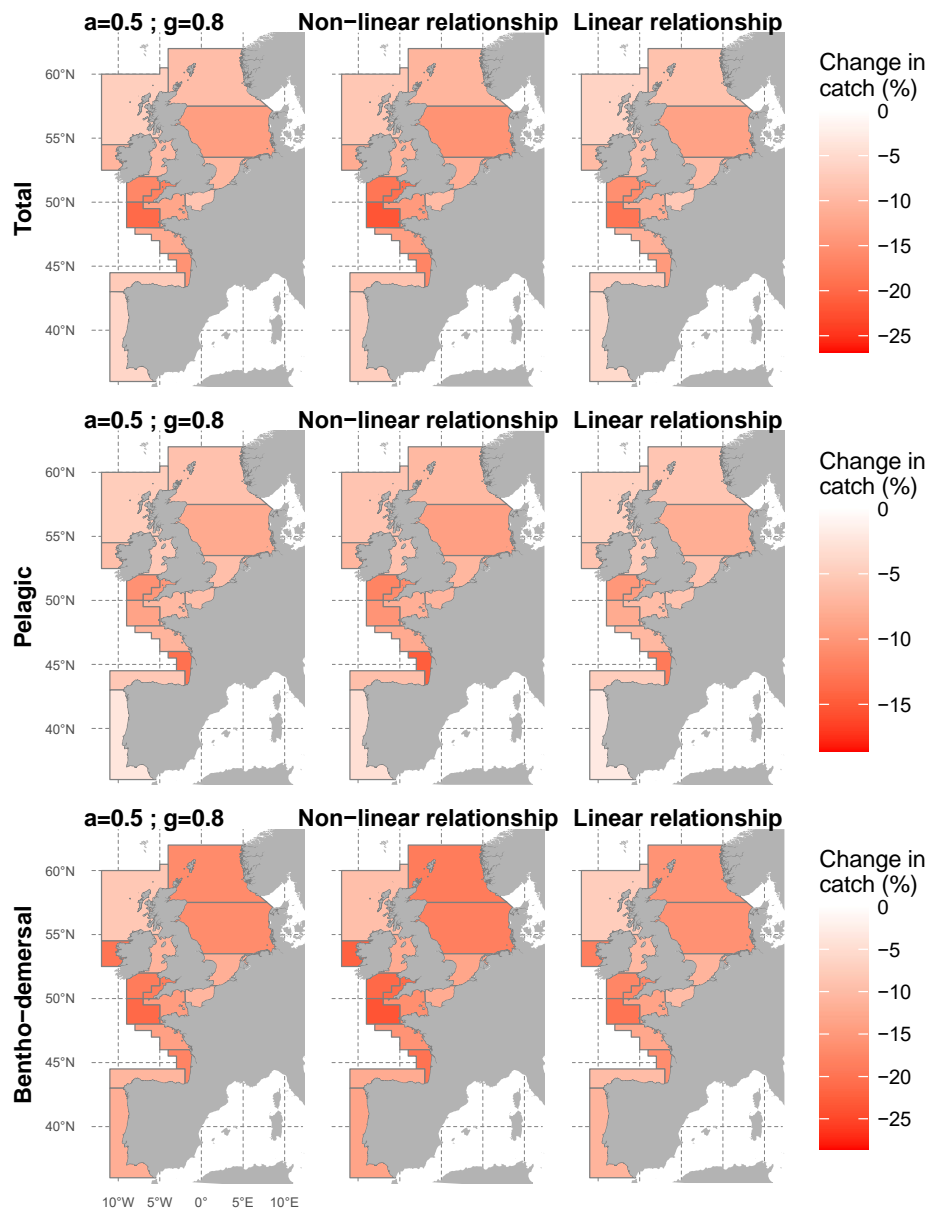


Figure S2.5: Maps of the changes in total catch in 2090–2099 relative to 2013–2017 under RCP8.5 for different predator-prey functional relationships in the top-down control function. The changes in total biomass ($TL \geq 2.5$) were aggregated for the entire ecosystem (top panels), the pelagic ecosystem component (center panels) and the benthо-demersal ecosystem component (bottom panels). Each column represents a top-down control intensity. Note that “ $a== 0.5$ and $g=0.8$ ” is the top-down control intensity ($\alpha=0.5$) and predator-prey functional relationship ($\gamma=0.8$), we used in the paper, “Linear relationship” represents the model with a linear predator-prey functional relationship ($\gamma=1$) and “Non-linear relationship” the model with a non-linear predator-prey functional relationship ($\gamma=0.5$).

Section S3.

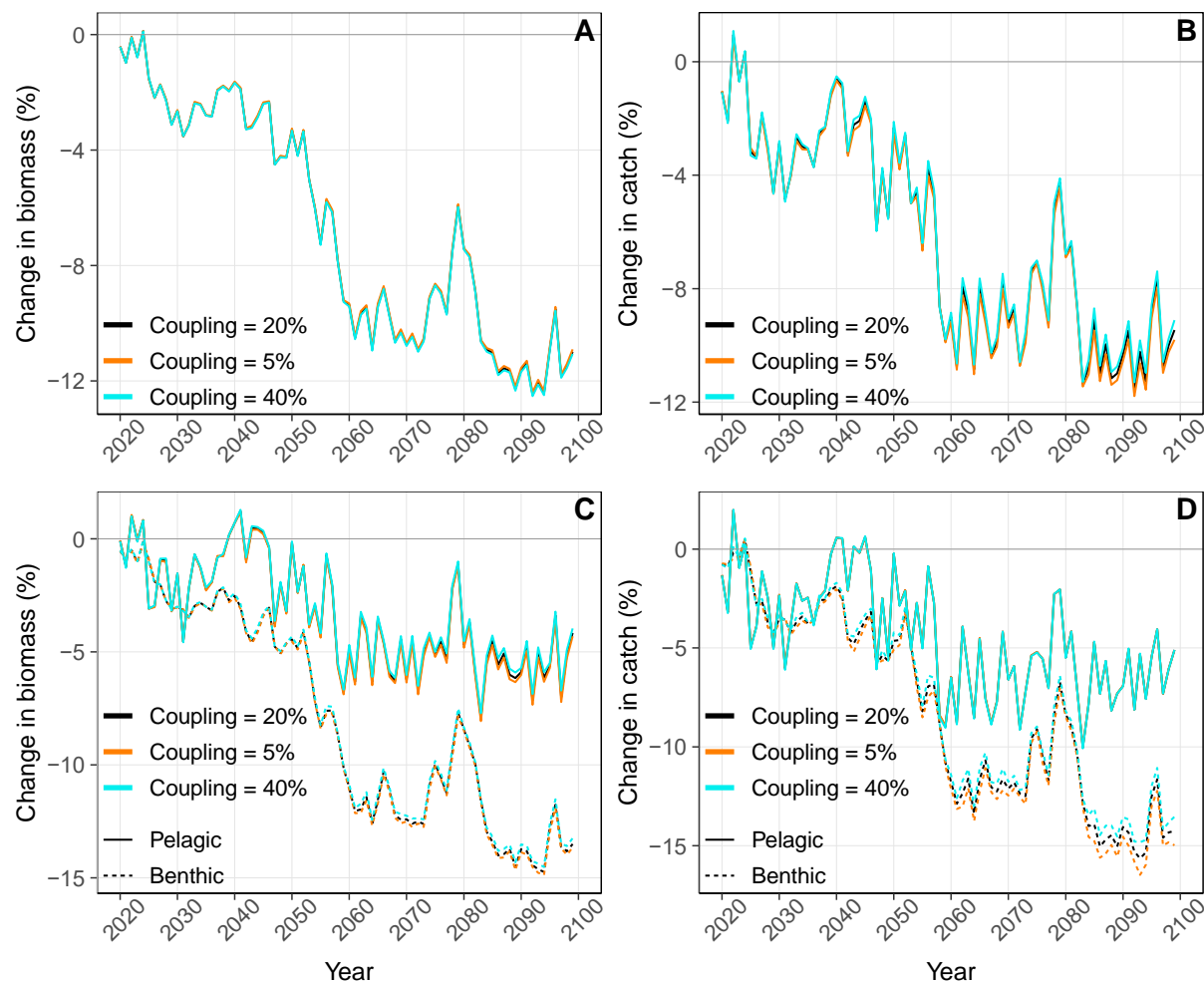


Figure S3.1: Projected biomass and catch from the European continental shelf trophic systems under RCP8.5 for three benthic-pelagic coupling scenarios. The projected change in total ($TL \geq 2.5$) biomass (A) and catch (B) between 2020 and 2100 relative to the reference period (2013–2017) are presented for two benthic-pelagic coupling scenarios. Panels (C) and (D) show the projected changes in biomass and catch for pelagic and benthic-demersal ecosystem components under RCP8.5 for two benthic-pelagic coupling scenarios. Note that “coupling = 20%” is the benthic-pelagic coupling scenarios used in our study.

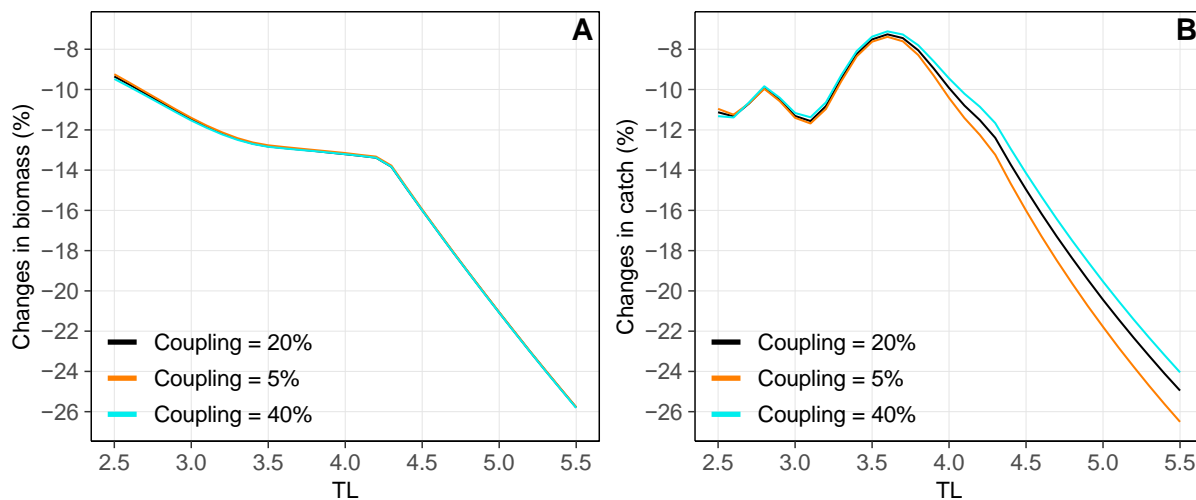


Figure S3.2: Projected changes in biomass and catch from the European continental shelf at each trophic level in 2090–2099 relative to 2013–2017 under RCP8.5 for three benthic-pelagic coupling scenarios. Note that “coupling = 20%” is the benthic-pelagic coupling scenarios used in our study.

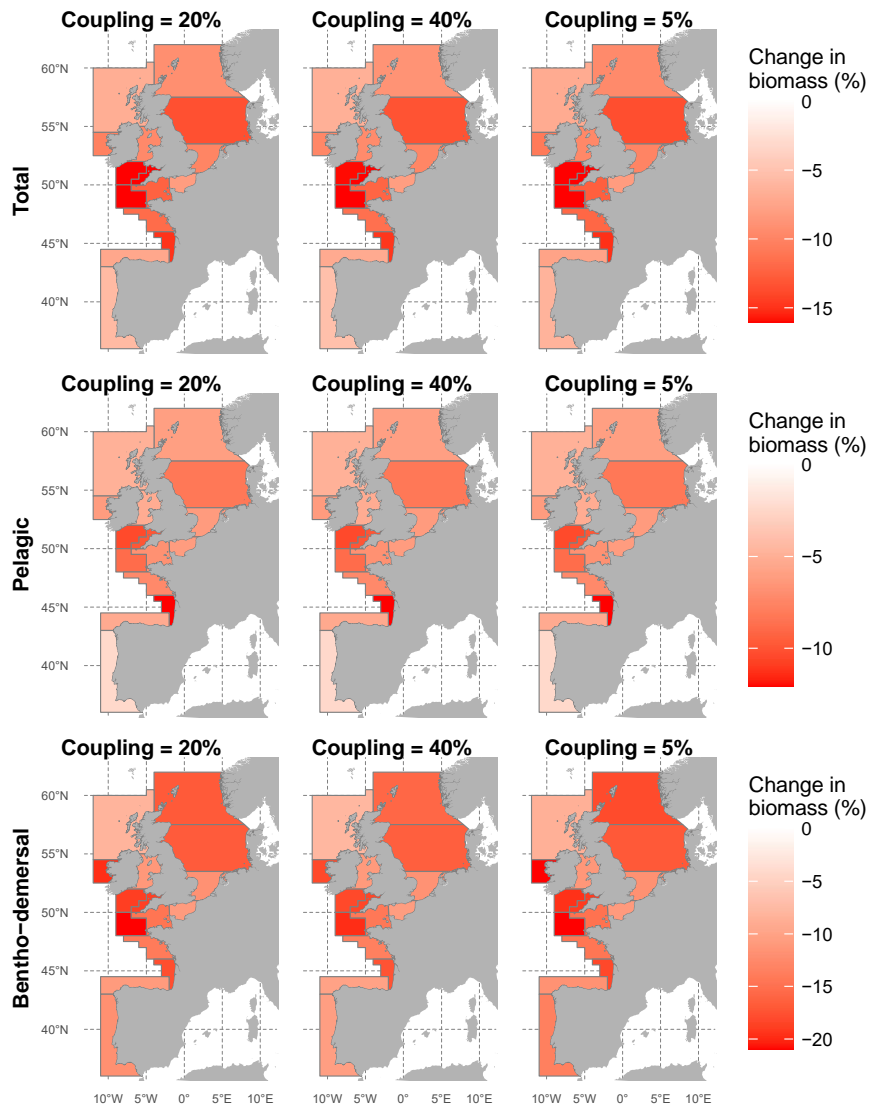


Figure S3.3: Maps of the changes in total biomass in 2090–2099 relative to 2013–2017 under RCP8.5 for three benthic-pelagic coupling scenarios. The changes in total biomass ($TL \geq 2.5$) were aggregated for the entire ecosystem (top panels), the pelagic ecosystem component (center panels) and the benthо-demersal ecosystem component (bottom panels). Each column represents a benthic-pelagic coupling scenarios. Note that “coupling = 20%” is the benthic-pelagic coupling scenarios used in our study.

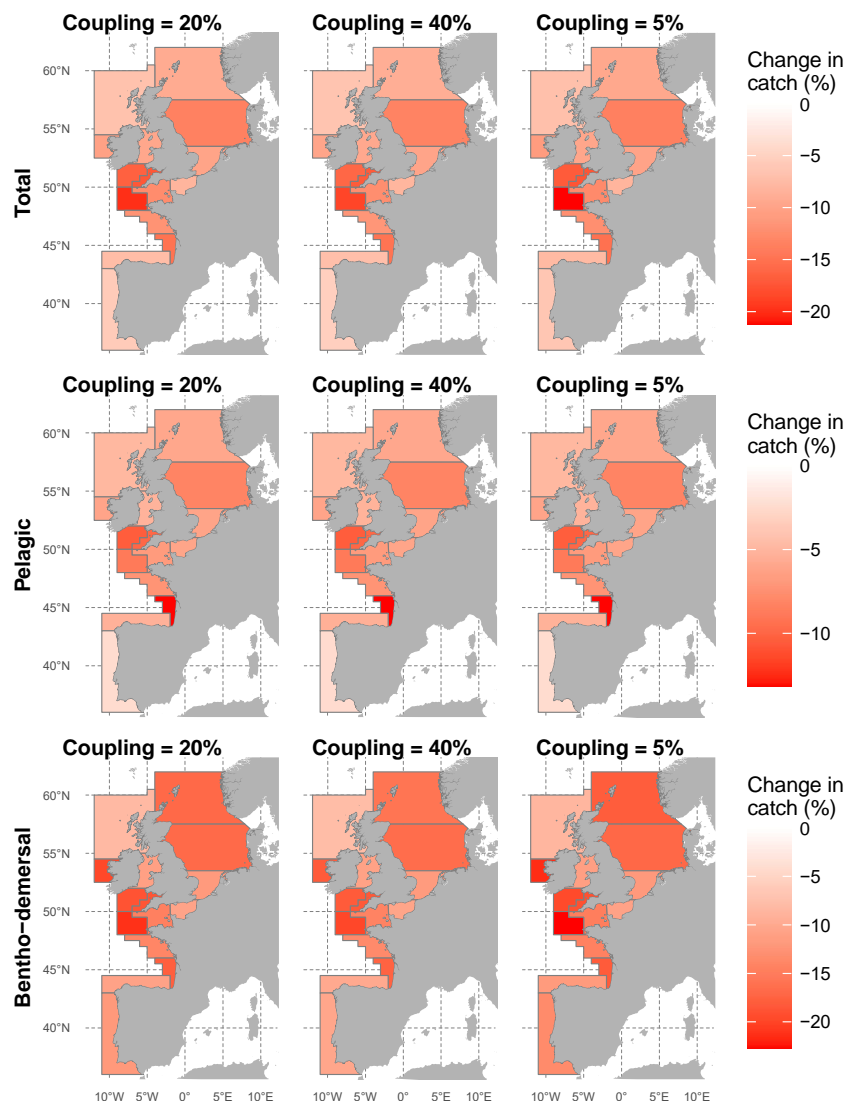


Figure S3.4: Maps of the changes in total catch in 2090–2099 relative to 2013–2017 under RCP8.5 for three benthic-pelagic coupling scenarios. The changes in total catch ($TL \geq 2.5$) were aggregated for the entire ecosystem (top panels), the pelagic ecosystem component (center panels) and the benthic-demersal ecosystem component (bottom panels). Each column represents a benthic-pelagic coupling scenarios. Note that “coupling = 20%” is the benthic-pelagic coupling scenarios used in our study.

Section S4.

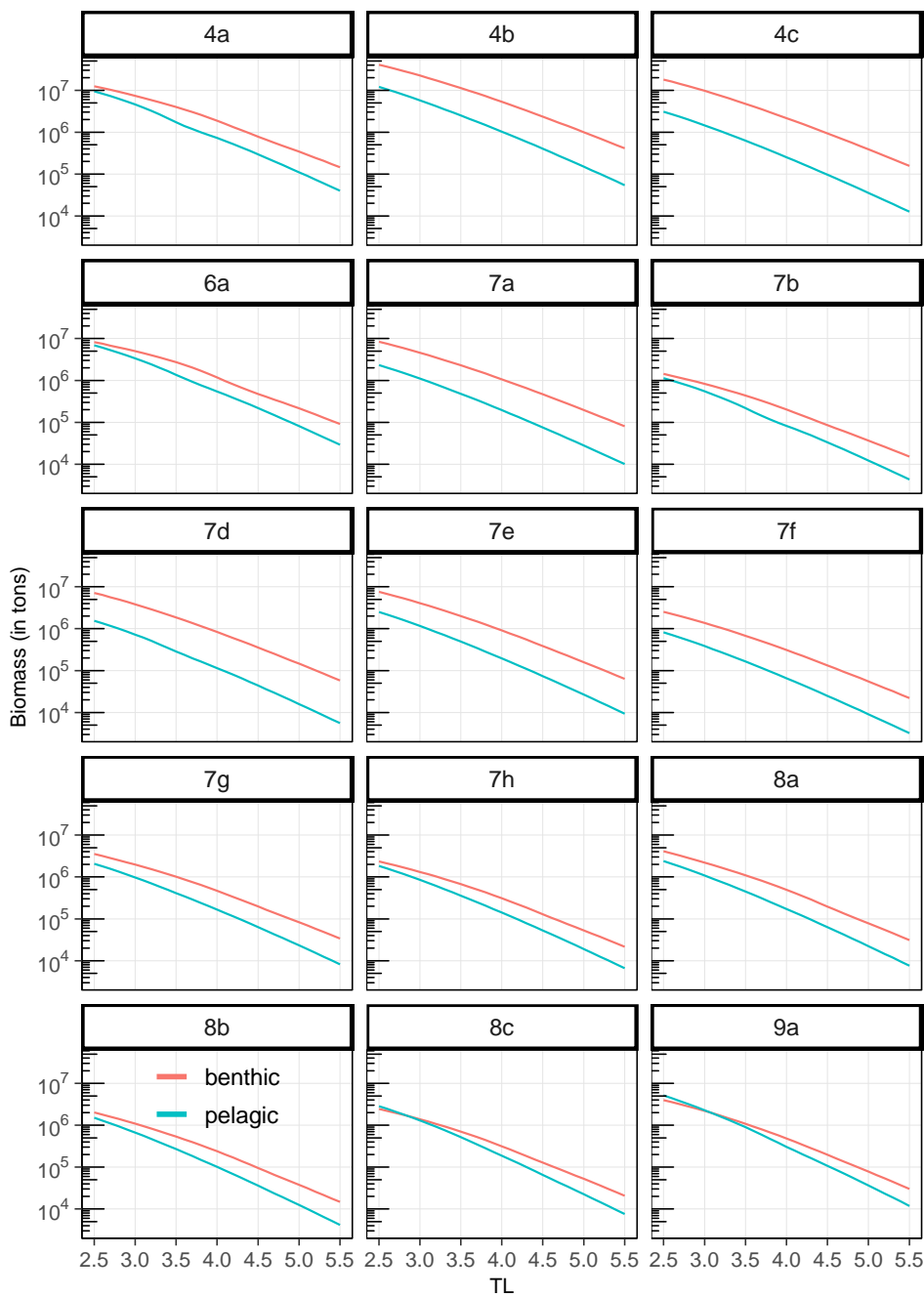


Figure S4.1: Biomass spectrum in each study area during the reference period 2013–2017.

Section S5.

Reference state of the 15 ICES divisions for the period 2013-2017

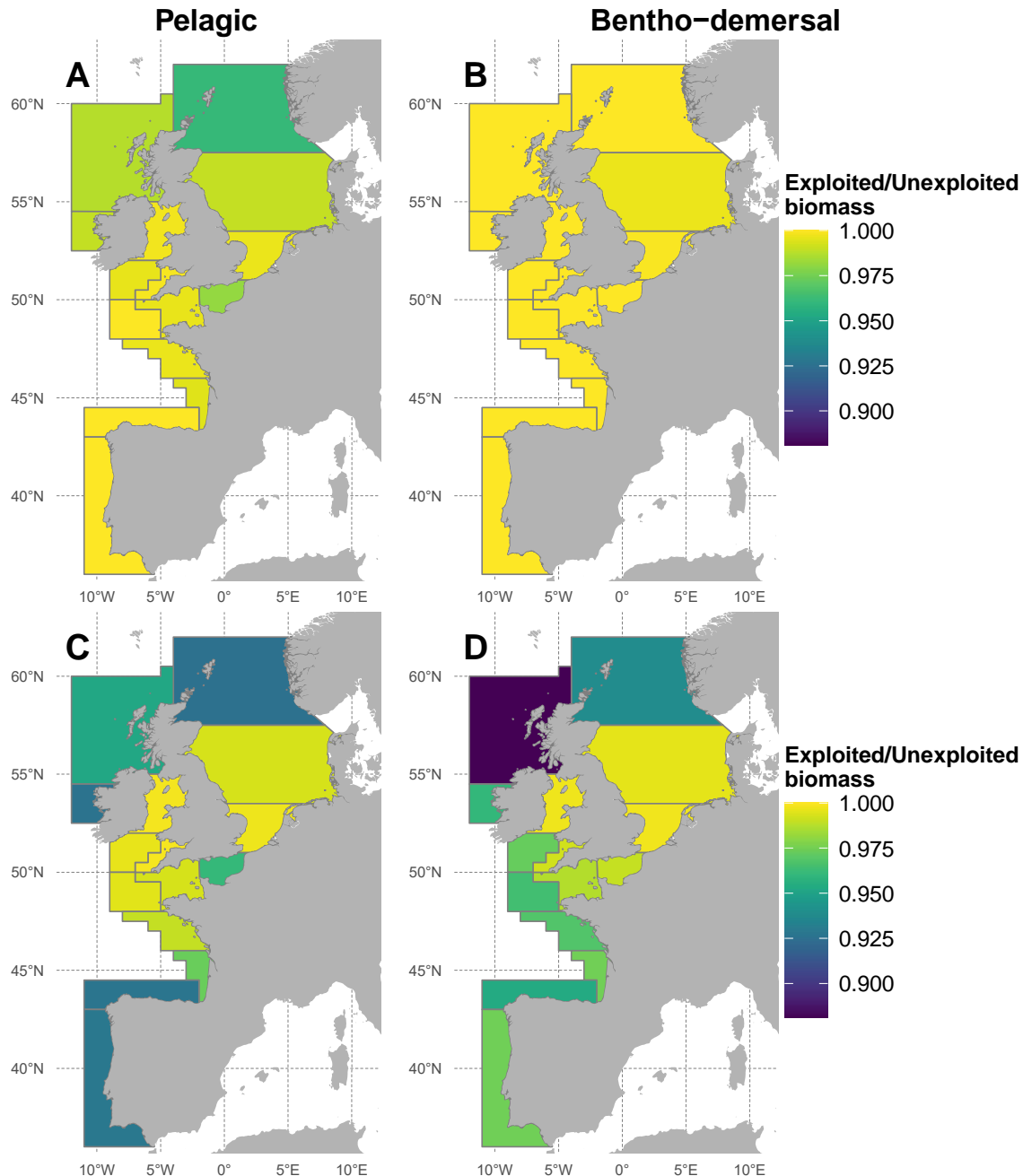


Figure S.5.1. Map of biomass ratio between exploited and theoretical unexploited ecosystems in 2017-2017 for the pelagic component (A and C) and for bentho-demersal component (B and D) as well as for lower trophic levels (between TL=3 and TL=4) (A and B) and for upper trophic levels (between TL=4 and TL=5.5) (C and D).

The ratios of exploited to unexploited pelagic biomass of the upper trophic levels (TLs) (between TL=4 and TL=5.5) vary between 1 and 0.92 (mean value at 0.97) and the ratios of exploited to unexploited benthic biomass vary between 1 and 0.88 (mean value at 0.97). The most impacted areas are the northernmost divisions (4a, 6a and 7b), the Eastern English Channel (7d) and southern division (8c and 9c). In parallel, the less affected areas are the Irish Seas (7a) and the South of the North Sea (4c). The biomass of the lower TLs between TL=3 and TL=4 appears very little affected by fishing with a mean ratio exploited/unexploited close to 1. At low TLs, biomass is even slightly enhanced by fishing due to a release of predation associated to a decrease in predators (3 ICES divisions out of 15 for the pelagic component and 7 out of 15 the benthic component).

All these biomass ratios must be analyzed cautiously because the fishing impacts appeared to be very low compared to the levels of impact found in the literature (Gascuel et al. 2016, Moullec et al. 2017, STECF 2020). However, this study does not aim to assess accurately the fishing impacts in 2013–2017. Instead, we defined a reference state in 2013–2017 to explore the effects of climate relative to this state.

- Gascuel D, Coll M, Fox C, Guénette S, Guitton J, Kenny A, Knittweis L, Nielsen JR, Piet G, Raid T, Travers-Trolet M, Shephard S (2016) Fishing impact and environmental status in European seas: a diagnosis from stock assessments and ecosystem indicators. Fish Fish 17:31–55.
- Moullec F, Gascuel D, Bentorcha K, Guénette S, Robert M (2017) Trophic models: What do we learn about Celtic Sea and Bay of Biscay ecosystems? J Mar Syst 172:104–117.
- STECF (2020) Scientific, Technical and Economic Committee for Fisheries (STECF): 62nd plenary meeting report (PLEN-19-03). Ulrich C, Doerner H (eds).